Robotic performance is comparable to human operators for cell therapy manufacturing tasks

Sudeshna Sadhu[1,*], Brigitte Schmittlein[1,*], Angela Lares[1], Sunaina Nayak[1], Marco Uboldi[2], Yifan Yu[3], Jiawei Wang[3], Wei Zhang[3], Prajakta P. Bhanap[4], Yongchang Ji[4], Andrew Scheffler[5], John Wilson[6], Dan Welch[6], Nikolaos Gkitsas-Long[7], Aidan Jeffery Retherford[7], Ramya Tunuguntla[7], Alice Melocchi[1,2,#], Federico Parietti[1], Steven A. Feldman[7], Jonathan H. Esensten[8]

[1] Multiply Labs, San Francisco, CA, USA.

[2] Sezione di Tecnologia e Legislazione Farmaceutiche "M. E. Sangalli", Dipartimento di Scienze Farmaceutiche, Università degli Studi di Milano, IT.

[3] GenScript Biotech Corporation, Piscataway, New Jersey, USA;

[4] Thermo Fisher Scientific, Carlsbad, California, USA;

[5] ScaleReady, New Brighton, Minnesota, USA;

[6] Wilson Wolf Manufacturing Corporation, New Brighton, Minnesota, USA;

[7] Center for Cancer Cell Therapy, Stanford Cancer Institute, Stanford University School of Medicine, Stanford, California, USA;

[8] The Advanced Biotherapy Center (ABC), Sheba Medical Center, Tel Hashomer, IL.

* These authors equally contributed to the work

[#] Corresponding author: 0039 0250324665; alice.melocchi@unimi.it

Keywords: robotic cluster; T cells; cell selection; harvest; cell counting; resuspension; sampling.

Abstract

Automation in cell therapy manufacturing has the potential to reduce labor costs, decrease variability, reduce contamination risks, and eliminate human errors while enabling rapid manufacturing scale-out. Here we show how a robotic system can precisely and robustly perform a wide variety of tasks (unit operations) common in cell therapy manufacturing. Each of these tasks can be combined by the robot in any order and any number to perform a specific manufacturing process. The robot uses existing modular equipment from market-leading vendors. In each case, we compare the performance of the robot to human operators and establish the accuracy and robustness of the robotic operations. We demonstrate comparability between human and robot for the following operations: bag-to-bag cell transfer, automated cell counting, drawing volume from a vial to a syringe, and cell resuspension and sampling from both a bag and G-Rex® 100M-CS bioreactor. Complex processes are also automated, including cell selection using a CytoSinct™ 1000 and wash/buffer exchange using a CTS™ Rotea™ Counterflow centrifugation system. Sterility was maintained during an aseptic process simulation incorporating several of the above unit operations for a generic CAR-T manufacturing process. These data demonstrate that a robotic system can efficiently perform specific unit operations required for the manufacture of a CAR-T drug product and, if linked, the above unit operations can be readily combined to rapidly automate processes that are currently entirely manual.

1. Introduction

Autologous effector cell-based therapies have demonstrated clinical efficacy in the treatment of cancer and autoimmune diseases [1-6]. The number of clinical trials for such therapies has dramatically increased: more than 3,000 trials were initiated over the last five years, with about 600 starting in 2023 alone [7-9]. The majority of autologous cell therapy trials were sponsored by pharmaceutical companies, highlighting the commercial potential and large market size.

However, current manufacturing approaches are difficult to scale out and are unlikely to be able to satisfy patient demand [10-12]. Current manufacturing of cell therapies in clean rooms requires multiple manual steps by highly trained operators [13,14]. This manual production strategy limits throughput and increases risk of errors and manufacturing failures [10]. Automation can improve robustness of manufacturing procedures and reduce costs [15-17]. Automated systems enhance productivity per unit area, allowing one employee to manage multiple automated systems at once.

Existing systems that automate one or multiple steps of the cell therapy manufacturing process were recently reviewed [18,19]. The two major approaches are *i)* all-in-one approach in which multiple steps are performed by a single device or *ii)* modular approach in which equipment from different vendors performs a single unit operation in series. All-in-one systems may be easier to use but harder to optimize and scale for new processes.

The modular approach allows easier customization, including incorporating newly available equipment or instruments intended for specific processes. There is also less reliance on a single supplier for any single task. Most importantly, modular workflows reduce the process constraints from the duration of the full process itself to the longest cycle-time of the isolated unit operations. This enables parallel processing and results in increased throughput capacity of each individual manufacturing line. Due to these advantages, a modular approach to cell therapy manufacturing has been extensively developed in both commercial and academic settings [20-26]. We have previously shown that a robotic cluster that uses industry-standard equipment can successfully culture CD8+ T cells with comparable cell yields, viability, and identity to those manually produced [27]. Here, we expand on that work and show the reliability and accuracy of specific common unit operations associated with CAR-T manufacturing as performed by a robotic system compared to a human operator. The performance of the robotic cluster is comparable to a human operator across a wide range of common cell therapy manipulations

including cell selection, buffer exchange, cell counting, and cell and/or medium transfer between vessels.

2. Materials and Methods

2.1 Modular robotic cluster

The robotic cluster consists of several modules, each of which is one cubic meter. These modules are accessed by a robotic arm mounted on a central rail (Figure 1).

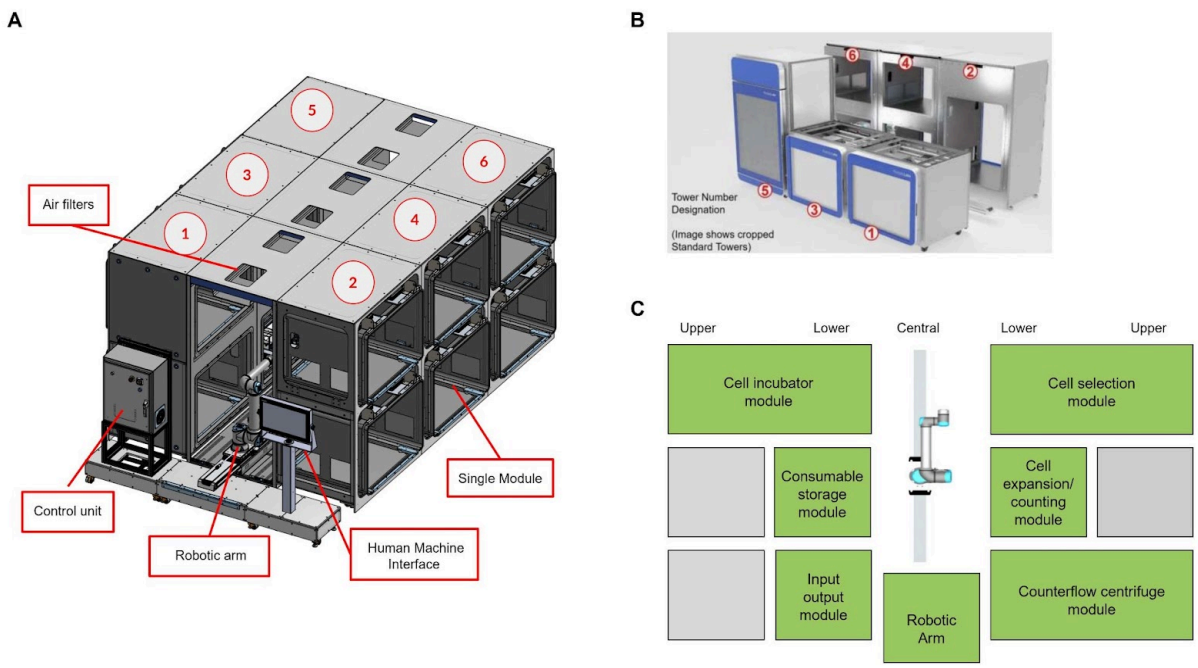

Figure 1. Schematics of the robotic cluster and modules. A) Outline of the robotic cluster. The image shows 6 towers: 1) Input output module, 2) Counterflow centrifuge module, 3) Consumable storage module, 4) Cell expansion/counting module, 5) Cell incubator module, 6) Cell selection module, B) Cut-out view of the robotic cluster. C) Representative diagram of the different towers/modules used in this study. Green denotes the modules in-use for this study and grey denotes idle modules.

This cluster represents an evolution of the system that was previously described [27]. The cluster walls have built-in air filter systems mounted on the top, which lower non-viable particles to ISO7 levels. Each module consists of standard equipment already used in Good Manufacturing Practices (GMP)-compliant manufacturing of cell therapies. The reagents or consumables required for each process were moved between modules using the robotic arm. Off-the-shelf consumables were purchased and assembled in-house to make them compatible with the robotic

arm. For example, syringes (5 and 10 mL; Becton Dickson) were attached to Texium™ connectors (Becton Dickson,10012241-0500), which in turn were assembled onto custom-designed couplers. The 1L transfer bags (Terumo, BB*T100BB71) and G-Rex® 100M-CS (Wilson Wolf Manufacturing Corporation, J81100-CS) were integrated into proprietary robotic cartridges. Vial cartridges were used to hold the vials assembled with proprietary vial adaptors. Similarly, the Via1-cassettes™ (Chemometec, 941-0011) for the NucleoCounter® NC-200™ automated cell counter (Chemometec), CytoSinct™ 1000 Tubing Set (GenScript Biotech Corporation, D00029) and the CTS™ Rotea™ Single-Use kit (Thermo Fisher Scientific, A49585) were purchased from the respective vendors and integrated into proprietary cartridges. The input/output module facilitated consumable addition and removal from the system. The cell incubator module contains a carbon dioxide incubator **(**Thermo Fisher Scientific, HERACELL VIOS 250i**)** capable of storing multiple G-Rex® 100M-CS bioreactors or cell culture bags. The cell expansion module contains hardware necessary for reagent transfer, cell transfer between bags and bioreactors, and sampling.

Experiments highlighted in Figure 2 were performed in the relevant module or modules. For vial-to-syringe fluid transfer operations, the consumable module includes stations and grippers for storing and manipulation of vials and syringes. The cell counting module features an automated NucleoCounter® NC-200™ (Chemometec) with a custom designed cartridge for sample dispensing and aspirating in the Via1-cassettes. For cell separation and enrichment, an enrichment/isolation module was used, containing a CytoSinct™ 1000 magnetic cell separation system (GenScript Biotech Corporation). For buffer exchange and cell harvest, a closed system centrifugation module was used, containing a CTS™ Rotea™ Counterflow centrifugation system (Thermo Fisher Scientific). The consumable kits and relevant bags were custom designed to be compatible with the robotic loading or unloading onto the CytoSinct™ 1000 or CTS™ Rotea™ equipment. Resuspension and sampling of cells can be conducted in different modules, provided the module includes a bag or bioreactor station. The robotic arm uses a gripper to pick up a bag or bioreactor, followed by mixing and resuspension of the bag or bioreactor via a rocking or shaking motion. The bioreactor or bag is then sampled from a port. The robotic cluster is designed to be modular to accommodate any combination of new instruments based on the unique needs of the manufacturing process.

2.2 Bag-to-Bag Cell Transfer

Human T cells (StemCell Technologies & AllCells) were seeded into an automation compatible permalife bag (OriGen, PL120-2G) in 100 mL TexMACS media. 24 hours post-seeding, cells were activated using TransAct (Miltenyi, 130-111-160). On day 3, cells were transferred from the permalife bag to the transfer pack (Fenwal Inc, 4R2001) robotically and the percentage of cells in each bag was assessed (Figure 2A).

2.3 Cell Counting

T cells were expanded and transferred into a bag at different concentrations. A 3.5 mL sample was drawn from the bag using a 10 mL syringe by either the robotic arm or a human operator (Figure 2B). The cells were loaded into a Via1-Cassette™. The robotic process used a specialized reservoir to perform the cell transfer from syringe to the counting cassette. Cell counts were performed in triplicate either manually or robotically using NucleoCounter® NC-200™.

2.4 Vial-to-Syringe Volume Draw

Each vial for robotic manipulation was attached to a 20 mm vented Vialok (Yukon) and SmartSite (Becton Dickinson) and then assembled to a proprietary vial adapter. Each vial was filled with 5 mL dyed water. For robotic conditions, the two filled vials were placed in the in-house designed vial cartridge. An empty 10 mL syringe with Texium™ connectors was attached to the coupler and placed in the designed syringe cartridge (Figure 2C). 4 mL was drawn from vial 1 and 1.8 mL was drawn from vial 2 using the same syringe to reach a target volume of 5.8 mL. Similarly, in the manual condition, 5.8 mL of fluid from two vials was pulled using the 10 mL syringe attached to the connector. The weight of the syringe for both conditions were measured manually and collected pre-draw (tare weight of the empty syringe), post-draw from vial 1, and again post-draw from vial 2 (Analytical Balance, Ohaus).

2.5 Cell Selection

Frozen or fresh apheresis was washed with phosphate buffered saline/EDTA (Miltenyi) containing 0.5% human serum albumin and incubated with CD4 and CD8 microbeads (Miltenyi)

for 30 minutes using LOVO® Cell Processing System (Fresenius Kabi). The labelled cells were equally divided into manual and robotic conditions for cell enrichment and isolation using the CytoSinct™ 1000 magnetic cell separation system (Figure 2D). TexMACS media supplemented with 3% serum, IL-7 and IL-15 was used as the buffer for enrichment. For manual conditions, the CytoSinct™ 1000 TS kit was set up per manufacturer's instructions. For robotic conditions, the kit and bags were assembled onto proprietary cartridges and loaded to the robotic cluster. For both manual and robotic conditions, $2x10^9$ target cells were loaded and Enrichment 1.1 protocol was performed. The cell count and viability pre-enrichment were provided by Stanford (Cellometer Auto 2000, Nexcelom Bioscience). Post-enrichment counts were assessed using NucleoCounter® NC-202™. To quantify T cell purity in the positive fraction, CD3+ T cells were measured by flow cytometry (BD LSR™ Fortessa, BD Biosciences or CytoFlexLX, Beckman Coulter) performed either at University of California San Francisco (UCSF) flow core or at Stanford University flow core. For each run, separate healthy donor apheresis was used.

2.6 Bag Resuspension and Sampling

Robotically enriched and expanded human T cells were harvested on day 8 post-activation from G-Rex® 100M-CS into a 1L transfer bag, resuspended, and sampled for cell counting (Figure 2E). Post-harvest, the cells in the bag were subjected to buffer exchange using the robotic CTS™ Rotea™ counterflow centrifugation system. The washed cells were then collected in another 1L transfer bag, resuspended, and sampled for cell counting. To accomplish robotic bag resuspension and sampling, the robot attached a syringe filled with 10 mL of sterile air to the 1L transfer bag to flush the tube line. Next, the bag was rocked for 2 minutes to mix the cells by tilting it up and down at a 30 degree angle from the horizontal position, with the syringe still attached. Following resuspension, the robot mixed the bag line with the syringe five times. A 2 mL sample was then removed from the bag using the same syringe. The sample and bag were then output from the robotic system and cell count was performed. The same 1L bag was then manually rocked for 2 mins by tilting it up and down at a 30 degree angle from the horizontal position, and a 2 mL sample was manually removed via syringe. All cell counts were performed manually using the NucleoCounter® NC-202™. This process was repeated on six different 1L transfer bags, with resuspension and sampling after G-Rex® 100M-CS transfer (n = 4) or post-Rotea (n = 2).

2.7 Bioreactor Resuspension and Sampling

Expanded primary human T cells were divided into four experimental conditions in different G-Rex® 100M-CS bioreactors, which included variations in cell number and volume: low cell number, low volume ($5.3x10^7$ cells in 100 mL medium), high cell number, high volume ($1.9x10^9$ cells in 600 mL medium), low cell number, high volume ($4.9x10^7$ cells in 600 mL medium), and high cell number, low volume ($1.3x10^9$ cells in 100 mL medium) (Figure 2F). The robotic cell resuspension protocol was designed to replicate the manual resuspension motion: a scientist from Stanford's Laboratory for Cell and Gene Medicine performed multiple resuspensions with motions recorded and translated to the robotic system using a motion capture system (Opitrak). After each resuspension, all conditions were allowed to rest for 2 hours to allow the cells to settle before the next resuspension.

2.8 Buffer Exchange and Cell Harvest

Enriched T cells were expanded and subjected to wash/buffer exchange using the CTS™ Rotea™ Counterflow centrifugation system (Figure 2G). The published buffer exchange protocol from Thermo Fisher Scientific was performed in both the manual and robotic conditions. However, prime volumes were increased in the robotic condition to account for the additional tubing length. Plasmalyte A containing 4% HSA was used as the buffer for both conditions. Cells were harvested in 40 mL of buffer.

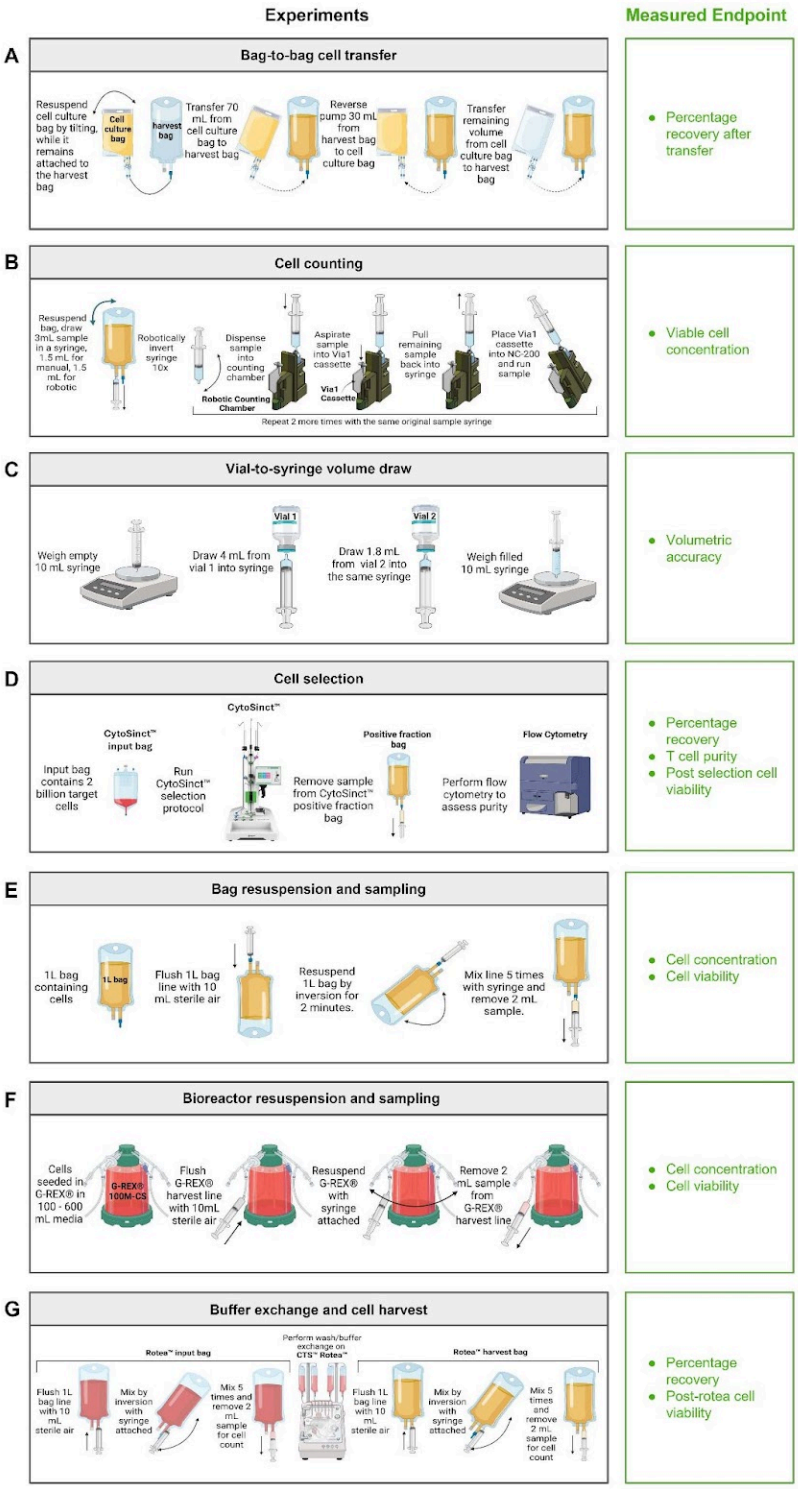

Figure 2. Outline of the various unit operations performed both manually and robotically. A) bag-to-bag cell transfer, B) cell counting, C) vial-to-syringe-volume draw, D) cell selection, E) bag resuspension and sampling, F) bioreactor resuspension and sampling, and G) buffer exchange and cell harvest. A video showing the various unit operations is included in the supplementary material (Video 1).

2.9 Aseptic Process Simulation (Media Fill) of a Robotic CAR-T Manufacturing Process

Aseptic process simulation was performed for a generic CAR-T cell manufacturing process. In the media fill experiment, the unit operations were performed sequentially and included transfer of volume between syringe and G-Rex® 100M-CS bioreactor, transfer of volume from bag to G-Rex® 100M-CS bioreactor, and resuspension of G-Rex® 100M-CS bioreactor. Baseline and dynamic environmental monitoring was performed at multiple locations inside the robotic cluster to determine environmental challenge conditions (Supplementary Table 1).

Sterile Tryptic Soy Broth media (Corning, MT46060CM) was transferred into pre-sterilized 1L transfer bags and containers needed for the process simulation in an ISO 5 biosafety cabinet (BSC). The prepared materials were then transferred into the robotic cluster via the input/output module. The filled media containers (n = 4), representing over 350 connections, media transfers, process additions and sampling, were checked for sterility in accordance with USP <71>. Post 14-day incubation media growth promotion testing was also performed.

To challenge the closed connection capability of the robotic clusters, the above aseptic process simulation was carried out under the worst possible conditions, *i.e.* having the unit self-contained HEPA/HVAC system purposefully non-operational.

2.10 Statistical Analysis

Graphpad Prism 10.4.0. were used to perform statistical analysis. Results are shown as mean ± Standard Deviation (SD) or mean ± Standard Error of Mean (SEM) and statistical differences between manual and robotic conditions were assessed by paired or unpaired Student's t-test. A two-tailed p value < 0.05 indicates a significant difference.

3. Results

In this study, we conducted parallel robotic and manual operations for each unit operation, with the exception of bag-to-bag cell transfer, and subsequently compared and analyzed the results.

3.1 Bag-to-Bag Cell Transfer

Bag-to-bag transfer is essential in cell therapy manufacturing for sterile, closed-system handling of biological materials. Cultured human T cells were transferred from a Permalife bag to a 150 mL transfer pack using a closed-loop pumping system with intermittent resuspension of the Permalife bag. Across three experiments, an average of 96% of viable cells were successfully transferred to the transfer pack, with 4% viable cells retained in the Permalife bag (Figure 3).

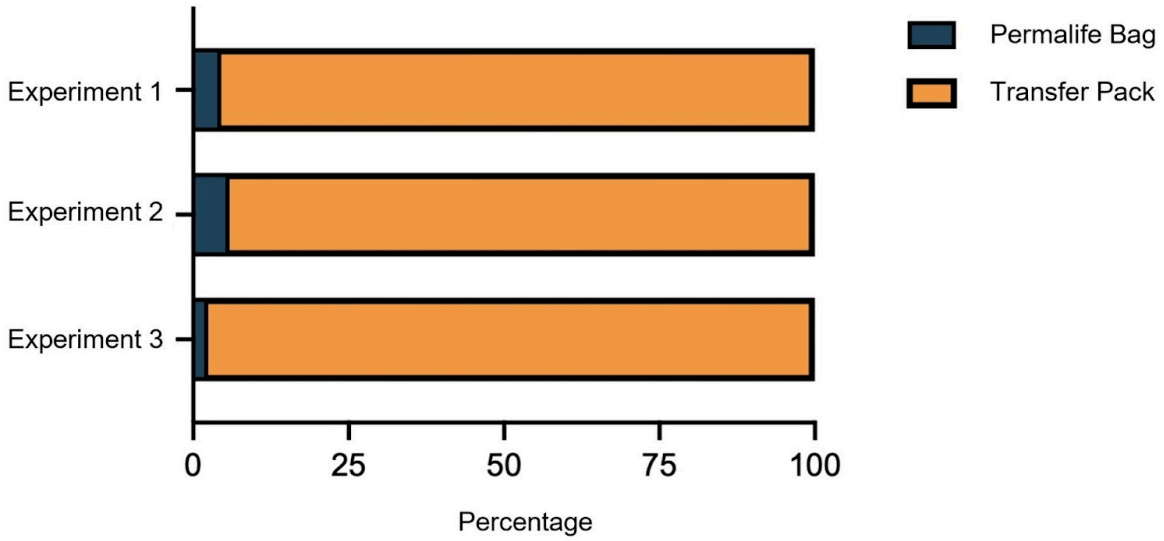

Figure 3. Automated bag-to-bag transfer of human T cells. Data is represented as the percentage of cells in each bag after the transfer was complete. n = 3 independent experiments.

3.2 Cell Counting

Human T cells were placed in bags at two concentrations: 3.5 - 4.0 x10^6 cells/mL ("high") and l5.3 - 6.1 x10^5 cells/mL ("low"). The cells were counted on a NucleoCounter® NC-200™ using

either a manual operator or a robotic process. The cell concentrations measured were comparable between manual and robotic approaches. For the high concentration, the average result was 3.74×10^6 cells/mL (manual, n = 15) and 3.69×10^6 cells/mL (robotic, n = 15) (Figure 4A). The coefficients of variation (CV) were also similar: 3.23% (manual) and 2.77% (robotic). Results were also comparable at the low concentration although a statistically significant lower count for the robotic condition was observed: 5.91×10^5 cells/mL (manual, n = 15) and 5.63×10^5 cells/mL (robotic, n = 15) (Figure 4B). The %CV was also comparable: 2.41% (manual) and 4.47% (robotic).

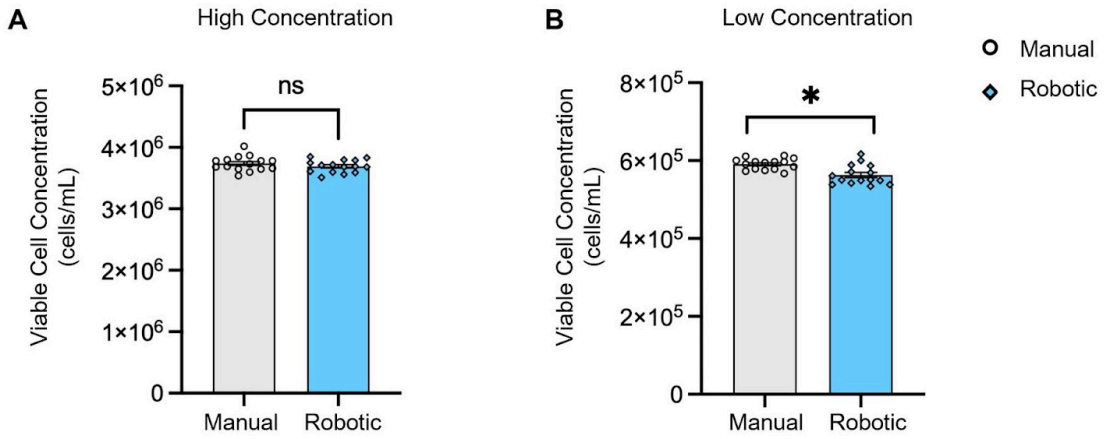

Figure 4: Comparison of manual versus robotic cell counts at high and low concentrations using a NucleoCounter® NC-200™ cell counter. A) Viable cell concentration at high concentration, B) Viable cell concentration at low concentration (unpaired t-test, for each concentration, n = 15 cell counts for manual and n = 15 cell counts for robotic). * indicates statistically significant results, $p<0.05$.

3.3 Vial-to-Syringe Volume Draw

Withdrawal of liquid from a reagent vial with a syringe is a routine task during cell therapy manufacturing. The accuracy of a vial-to-syringe draw was assessed using off-the-shelf glass vials and 10 mL syringes. An arbitrary target volume of 5.8 mL was chosen as the total draw volume from two vials. The average draw volume for the manual condition was 5.55 mL and 5.62 mL for the robotic condition (Figure 5A). The accuracy was slightly higher in robotic draws compared to manual draws (Figure 5A, 5B). There was considerable overlap in the difference from the target volume between the manual and robotic conditions (Figure 5C).

After additional calibration of the robotic system to account for dead volume in the syringe hub, an additional experiment was performed. The target volume remained 5.8 mL. The average volume for the manual conditions was 5.94 mL and for the robotic condition 5.97 mL (Figure 5D). Both the manual and robotic conditions were able to achieve a draw volume slightly above the target volume (Figure 5E).

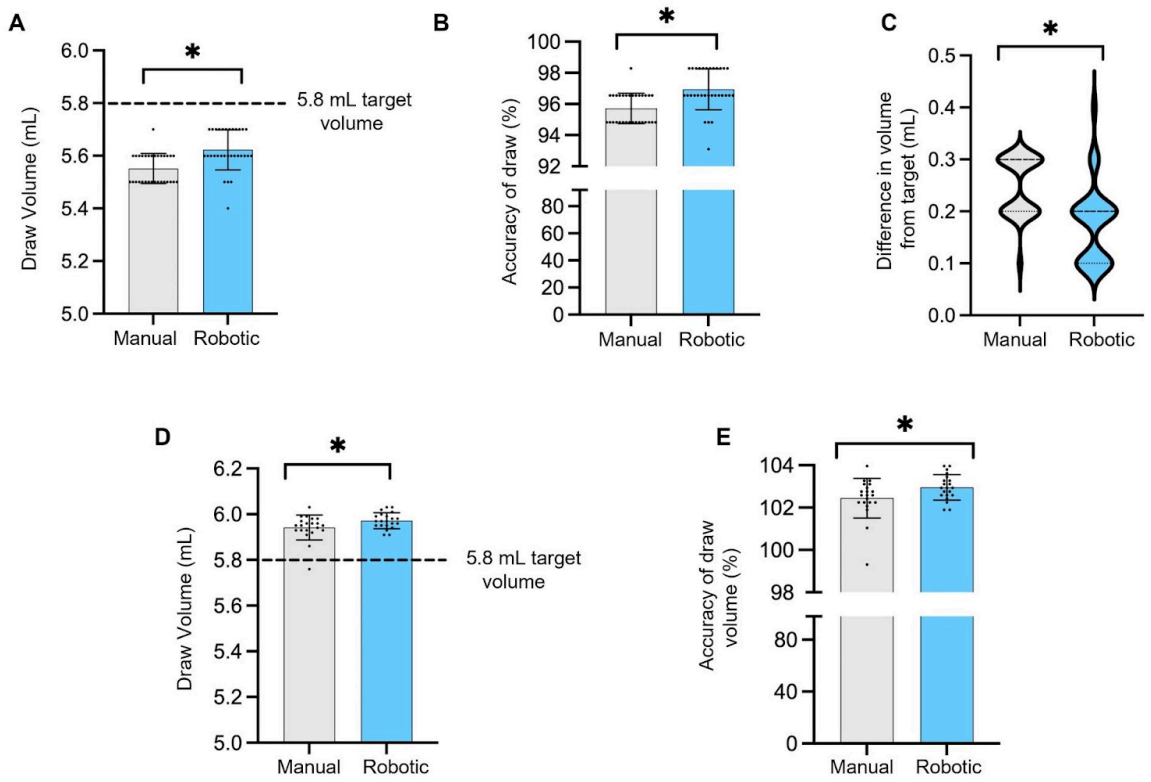

Figure 5. Accuracy of vial-to-syringe draw in manual and robotic conditions. A-C shows initial calibration conditions (unpaired t-test. n = 31). D-E shows modified calibration conditions (unpaired t-test, n = 20).* indicates statistically significant results, $p<0.05$.

3.4 Cell Selection

We performed a concurrent manual (n = 5) and robotic (n = 6) positive selection of T cells using a CytoSinct™ instrument and the CytoSinct™ 1000 TS tubing kit. Frozen apheresis was thawed, washed, and incubated with CD4 and CD8 microbeads. The target cell input range was $0.5x10^9$-

$2.0x10^9$ cells. Post-selection, the total T cell yield recovery was comparable between manual and robotic conditions, although greater variability was observed in the robotic condition compared to manual (Figure 6A).

Post-selection T cell purity was assessed by flow cytometry (Figure 6B). The percentage of CD3+ T cells in the positive fraction was comparable between conditions, and above 80% in all runs. Post-selection cell viability was quantified in the positive fraction for both the manual and robotic processes (Figure 6C). Comparable results for cell viability were observed in both processes. Other cell subsets were also quantified (Supplementary Figure 1).

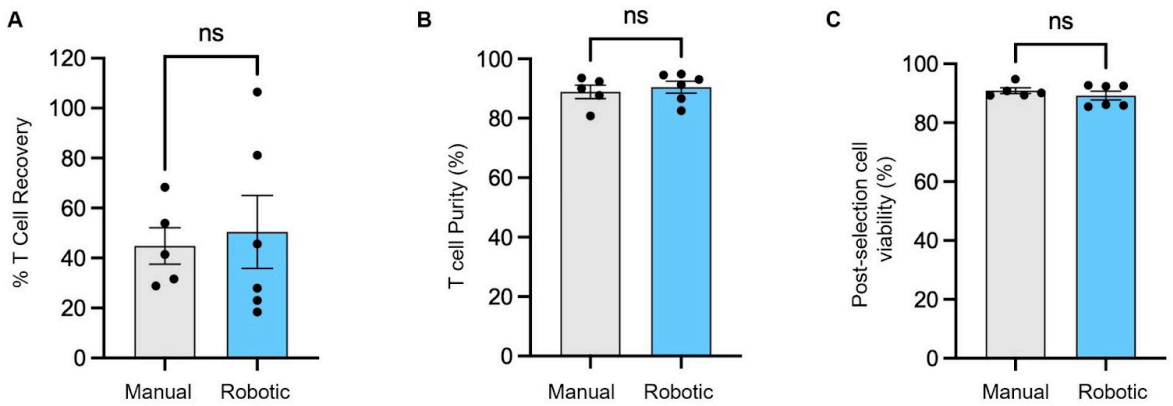

Figure 6. T cell recovery and purity comparison between manual and robotic selection using a CytoSinct™ 1000 magnetic cell separation system. A) Percent recovery of T cells in the positive fraction compared to the starting material, B) post-selection T cell purity in the positive fraction, and C) post-selection cell viability. Statistical comparisons are an unpaired t-test, ns = non-significant. n = 5 for manual condition and n = 6 for robotic condition.

3.5 Bag Resuspension and Sampling

Primary human T cells at low ($1x10^6$ cells/mL) and high ($20x10^6$ cells/mL) concentrations were placed in 50 - 300 mL volumes in 1L bags. The bags were resuspended by manual or robotic mixing. The bags were then sampled and counted (Figure 7). On average, across six runs, the cell counts after robotic mixing were within 5.4% of the manual process average counts.

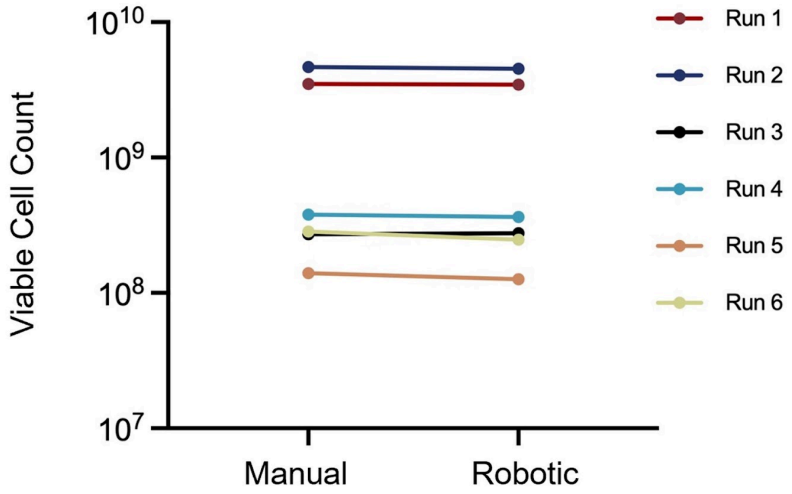

Figure 7. Manual *versus* robotic resuspension of human T cells in a 1L transfer bag. Viable cell counts post resuspension were measured.

3.6 Bioreactor Resuspension and Sampling

Primary human T cells in two volumes (100 versus 600 mL) and a range of cell concentrations ($0.08x10^6$ - $13.7x10^6$ cells/mL) were placed into a G-Rex® 100M-CS bioreactor. The cells were allowed to settle for 2 hours and then resuspended manually or robotically with a swirling motion. Cells were then sampled and counted. Averaged manual and robotic cell counts from 3 replicates across four conditions showed comparable results between manual and robotic methods, with less than 2% difference in each comparison (Figure 8).

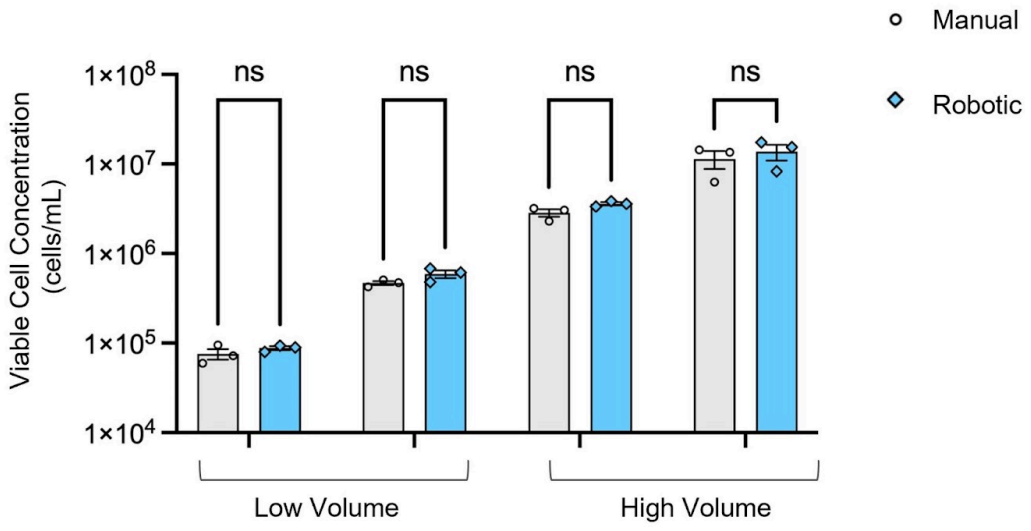

Figure 8: Manual *versus* robotic resuspension of cells in a bioreactor. Cells at different concentrations and volumes in a G-Rex® 100M-CS bioreactor were resuspended with manual or robotic swirling motion. Cell concentration was then measured (unpaired t-test, n = 3).

3.7 Buffer Exchange and Cell Harvest

The CTS™ Rotea™ Counterflow centrifugation system has several functions, including volume reduction and buffer exchange. We compared manual versus robotic buffer exchange using the Rotea and primary human T cells (ranging from $0.2x10^9$ to $4.0x10^9$) in independent runs. The cell recovery for the manual process ranged from 83% to 95%, while the cell recovery for the robotic process ranged from 81% to 133% (Figure 9A). The cell viability post-harvest was above 93% in the manual condition, whereas in the robotic condition, viability ranged from 83% to 97% (Figure 9B). There was no significant difference in percent cell recovery or post-harvest cell viability between manual and robotic conditions.

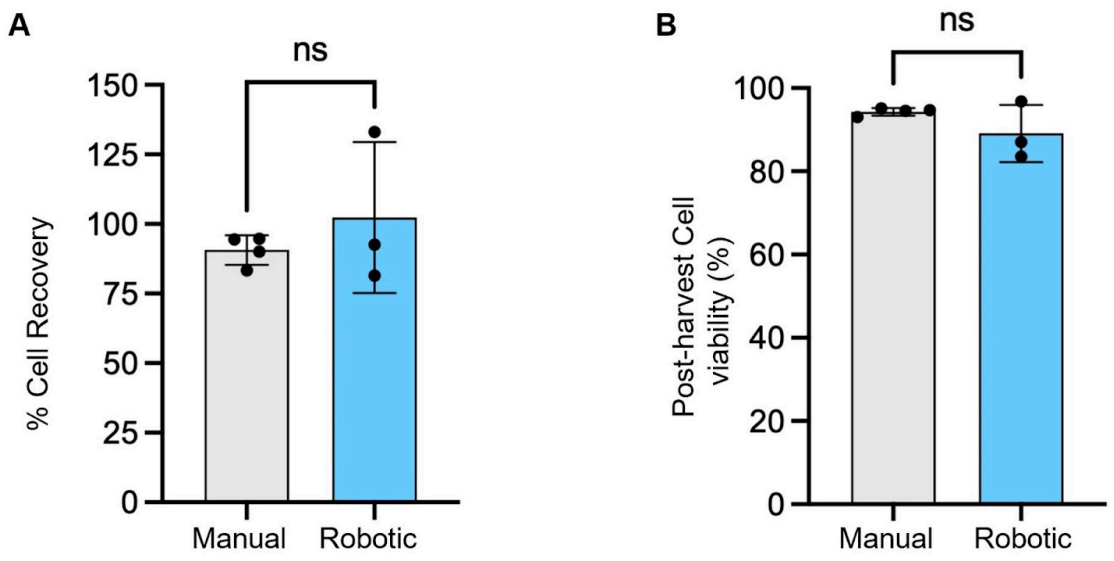

Figure 9: Comparison of Manual and Robotic Harvest Processes Using the CTS™ Rotea™ Counterflow Centrifugation System. A) percentage cell recovery, and B) post-harvest total cell viability (unpaired student's t-test, non-significant difference between manual and robotic condition. n = 4 for manual and n = 3 for robotic).

3.8 Aseptic Process Simulation (Media Fill) of a Robotic CAR-T Manufacturing Process

To confirm the ability of the robotic system to maintain sterility during cell manipulations, aseptic process simulations were carried out for a generic CAR-T cell manufacturing process. No bacterial growth was observed in the media after 14 days of incubation at 37 °C or longer (Table 1). Notably, the robotic system was found to maintain sterility of the process when placed in a standard research laboratory space (non classified environment). An analysis of viable and non-viable particles inside the laboratory space is presented in Supplementary Table 1.

Experiment types	Runs	14-day sterility test (Growth / No Growth)	Pass / Fail
Media fill	**1**	**No growth**	**Pass**
	2	**No growth**	**Pass**
	3	**No growth**	**Pass**
	4	**No growth**	**Pass**

Table 1: Aseptic process simulation results using robotic unit operations for a generic effector T cell manufacturing process.

4. Discussion

The robotic system achieves comparable accuracy and precision to the human operator while manipulating instruments and consumables that were designed for human hands. This data lays the foundation for demonstrating full end-to-end automation of the complete manufacturing processes for cell and gene therapies under cGMP.

In some cases, such as resuspension of cells in a G-Rex® 100M CS bioreactor, the robotic motions were based on motion capture from a human operator. The bag resuspension motion, by contrast, involved a simple back and forth tilting enabled by a robotic joint rotation, and was not defined by human motion patterns. Optimizing these motions for the robot and for the specific cell type being handled is a key area of improvement. Robotic systems are ideally suited to explore the large parameter space of such specific motions that cannot be reliably or accurately reproduced by human operations in different manufacturing sites.

We did not demonstrate the precision and accuracy of large volume transfer (>100 mL) from one vessel to another. The ability of a robot to precisely transfer specific large volumes relies on multiple systems including accurate peristaltic pumps and closed loop weights for both the origin and destination vessels. These improvements are planned for further development.

In addition, small volumes are also challenging for the robot. Drawing volume into a syringe from a vial represents another focus area of work because this simple unit operation is required

for adding growth factors or other high cost, low volume reagents to a culture. Our results showed that this process requires proper calibration to achieve accuracy. This calibration should take into account viscosity and surface tension of the liquid involved, the relevant dead volumes in the consumables, and the specific sizes of the consumables.

In the cell counting unit operation, the robot dispenses samples from a syringe into a custom chamber, which is then used as a vessel to load a Via1-cassette™ for the NucleoCounter® NC-200™ cell counter. The robotic system is designed to mitigate cell settling by mixing the sample between counts (via inversion), ensuring homogenous cell suspension. Despite this, we did see a statistically significant but biologically negligible difference in the cell counts at the lower concentration. This difference was seen due to the high precision of the multiple replicates performed on this unit operation. The difference may be due to the different handling of the sample between the robot and human operators, and it is uncertain if the robotic count or the manual count is more accurate.

For cell isolation, we demonstrated the CytoSinct™ 1000 magnetic cell separation system for T cell enrichment from leukapheresis products, comparing manual and robotic processing methods. Automating this instrument was deemed the best choice as it is not limited to T cell enrichment, and can be used for isolation, enrichment and depletion of other cell types like hematopoietic stem cells, NK cells, and other cell types. To improve recovery in the robotic runs, collaboration with GenScript resulted in a few iterations of the Enrichment 1.1 protocol, involving changes such as increasing the washing/elution time. Similar optimizations are likely to be required for instruments with large, dedicated tubing sets. The CTS™ Rotea™ Counterflow Centrifugation System has many functions including washing, diluting, volume reducing, aliquoting, and media exchange. This flexibility allows for the application of the automation work done here to be applied to other unit operations relying on the same instrument. In one run, the cell recovery was greater than 100%. This result may be related to cell clumps that formed during culture that were subsequently reduced to single cells during processing.

Importantly, all unit operations need to be done under conditions that maintain sterility of the product. The robotic system uses multiple-use needle free connectors, which were sanitized with alcohol-containing disinfecting caps before each use. Since all activities occur inside of the

robotic cluster without human intervention, the risk of contamination is reduced compared to a manual process with human operators performing the same functions in a cleanroom. This would enable a lower cleanroom classification (*e.g.* an ISO 7 *versus* an ISO 5). Future optimization of the robotic cluster will be aimed at improving efficiency and quality via iterations on the system hardware and software. Furthermore, as the robotic actions become more reliable, their processing rate could be increased, thus decreasing the overall time of operation. In parallel, standardization, optimization, and mass production of the robotic adapters for each consumable and piece of equipment is required to be able to scale out the system to commercially relevant numbers.

5. Conclusions

Robotic automation has the potential to replace many highly manual procedures using standard equipment that was designed for use by human hands. End-to-end automation of a modular manufacturing process can increase the supply of cell therapy products to meet global demand, improve efficiency, accelerate delivery timelines, and ensure high quality standards are consistently met.

Acknowledgement

We would like to express our gratitude to ChemoMetec, Akron Bio and Cytiva, for technical advice and feedback during the work.

References

1. De Marco R.C., Monzo H.J., Ojala P.M., 2023, CAR T cell therapy: a versatile living drug, Int. J. Mol. Sci., 24: 6300. https://doi.org/10.3390/ijms24076300
2. Fugger L., Torp Jensen L., Rossjohn J., 2020, Challenges, progress, and prospects of developing therapies to treat autoimmune diseases, Cell, 181: 63-80. https://doi.org/10.1016/j.cell.2020.03.007.

3. Greco R., Alexander T., Del Papa N., Müller F., Saccardi R., Sanchez-Guijo F., Schett G., Sharrack B., Snowden J.A., Tarte K., Onida F., Sánchez-Ortega I., Burman J., Castilla Llorente C., Cervera R., Ciceri F., Doria A., Henes J., Lindsay J., Mackensen A., Muraro P.A., Ricart E., Rovira M., Zuckerman T., Yakoub-Agha I., Farge D., 2024, Innovative cellular therapies for autoimmune diseases: expert-based position statement and clinical practice recommendations from the EBMT practice harmonization and guidelines committee, eClinicalMedicine : 69: 102476. https://doi.org/10.1016/j.eclinm.2024.102476
4. Gustafson M.P., Ligon J.A., Bersenev A., McCann C.D., Shah N.N., Hanley P.J., 2023, Emerging frontiers in immuno- and gene therapy for cancer, Cytotherapy, 25:20-32. https://doi.org/10.1016/j.jcyt.2022.10.002
5. Park Y., Kwok S.K., 2022, Recent advances in cell therapeutics for systemic autoimmune diseases, Immune Netw., 22:e10. https://doi.org/10.4110/in.2022.22.e10
6. Wang L., Liu G., Zheng L., Long H., Liu Y., 2023, A new era of gene and cell therapy for cancer: a narrative review, Ann Transl Med., 11:321. https://doi.org/10.21037/atm-22-3882
7. Arabi F., Mansouri V., Ahmadbeigi N., 2022, Gene therapy clinical trials, where do we go? An overview, Biomedicine & Pharmacotherapy, 153: 113324 https://doi.org/10.1016/j.biopha.2022.113324.
8. Ginn S.L., Mandwie M., Alexander I.E., Edelstein M., Abedi M.R., 2024, Gene therapy clinical trials worldwide to 2023- An update, J. Gene Med., 26: e3721. https://doi.org/10.1002/jgm.3721
9. https://www.iqvia.com/insights/the-iqvia-institute/reports-and-publications/reports/strengthening-pathways-for-cell-and-gene-therapies, last access on January 22, 2025
10. Ayala Ceja M., Khericha M., Harris C. M., Puig-Saus C., Chen Y. Y., 2024, CAR-T cell manufacturing: Major process parameters and next-generation strategies, J. Exp. Med., 221: e20230903. https://doi.org/10.1084/jem.20230903
11. Heathman T.R., Nienow A.W., McCall M.J., Coopman K., Kara B., Hewitt C.J., 2015, The translation of cell-based therapies: clinical landscape and manufacturing challenges, Regen. Med., 10: 49-64). https://doi.org/10.2217/rme.14.73

12. Iancu E.M., Kandalaft L.E, 2020, Challenges and advantages of cell therapy manufacturing under Good Manufacturing Practices within the hospital setting, Cur. Opin. Biotechnol., 65: 233-241. https://doi.org/10.1016/j.copbio.2020.05.005
13. Campbell A., Brieva T., Raviv L., Rowley J., Niss K., Brandwein H., Oh S., Karnieli O., 2015, Concise review: Process development considerations for cell therapy. Stem Cells Transl. Med., 4:1155-1163. https://doi.org/10.5966/sctm.2014-0294
14. Lee N.K., Chang J.W., 2024, Manufacturing cell and gene therapies: challenges in clinical translation. Ann. Lab. Med., 44: 314-323. https://doi.org/10.3343/alm.2023.0382
15. Brindley D. A., Wall, I. B., Bure K. E., 2013, Automation of cell therapy biomanufacturing minimizing regulatory risks and maximizing return on investments, BioProcess Int., 11: S42-S49.
16. Doulgkeroglou M. N., Di Nubila A., Niessing B., König N., Schmitt R. H., Damen J., Szilvassy, S. J., Chang W., Csontos L., Louis S., Kugelmeier P., Ronfard V., Bayon Y., Zeugolis D. I., 2020, Automation, monitoring, and standardization of cell product manufacturing, Front. Bioeng. Biotechnol., 8: 811. https://doi.org/10.3389/fbioe.2020.00811
17. Smith D., Heathman T. R. J., Klarer A., LeBlon C., Tada Y., Hampson B., 2019, Towards automated manufacturing for cell therapies, Curr. Hematol. Malig. Rep., 14: 278-285. https://doi.org/10.1007/s11899-019-00522-y
18. Melocchi A., Schmittlein B., Sadhu S., Nayak S., Lares A., Uboldi M., Zema L., di Robilant B., ì Feldman S.A., Esensten J.H., 2025, Automated manufacturing of cell therapies, J. Control. Release, 381:113561. https://doi.org/10.1016/j.jconrel.2025.02.057
19. Moutsatsou P., Ochs J., Schmitt R. H., Hewitt C. J., Hanga M. P., 2019, Automation in cell and gene therapy manufacturing: from past to future. Biotechnol. Lett., 41: 1245–1253. https://doi.org/10.1007/s10529-019-02732-z
20. Franscini N., Wuertz K., Patocchi-Tenzer I., Durner R., Boos N., Graf-Hausner Ursula U., 2011, Development of a novel automated cell isolation, expansion, and characterization platform, J. Lab. Autom., 16: 204-213. https://doi.org/10.1016/j.jala.2011.01.002
21. Kami D., Watakabe K., Yamazaki-Inoue M., Minami K., Kitani T., Itakura Y., Toyoda M., Sakurai T., Umezawa A., Gojo S., 2013, Large-scale cell production of stem cells for

clinical application using the automated cell processing machine. BMC Biotechnol., 13: 102. https://doi.org/10.1186/1472-6750-13-102

22. Kikuchi, T., Kino-oka, M., Wada, M., Kobayashi, T., Kato, M., Takeda, S., Kubo, H., Ogawa, T., Sunayama, H., Tanimoto, K., Mizutani, M., Shimizu, T., Okano, T. (2018). A novel, flexible and automated manufacturing facility for cell-based health care products: Tissue Factory. Regenerative Therapy, 9, 89–99. https://doi.org/10.1016/j.reth.2018.08.004
23. Mantripragada V.P., Luangphakdy V., Hittle B., Powell K., Muschler G.F., 2020, Automated in-process characterization and selection of cell-clones for quality and efficient cell manufacturing, Cytotechnol., 72:615-627. https://doi.org/10.1007/s10616-020-00403-w
24. Murphy M., Barry F., Leschke C., Vaughan B., Gentili C., O'Dea J., Ogourtsov V., Rafiq Q. A., Ochs J., Kulik M., Koenig N., 2017, The autostem platform for closed manufacture of bone marrow-derived mesenchymal stromal cells using a closed, scalable and automated robotic system, Cytotherapy, 19:, s122. https://doi.org/10.1016/j.jcyt.2017.02.199
25. Rafiq Q.A., Twomey K., Kulik M., Leschke C., O'Dea J., Callens S., Gentili C., Barry F. P., Murphy M., 2016, Developing an automated robotic factory for novel stem cell therapy production, Regen. Med., 11: 351-354. https://doi.org/10.2217/rme-2016-0040
26. Thomas R.J., Chandra A., Liu Y., Hourd P.C., Conway P.P., Williams D.J., 2007, Manufacture of a human mesenchymal stem cell population using an automated cell culture platform, Cytotechnol., 55: 31-39. https://doi.org/10.1007/s10616-007-9091-2
27. Melocchi A., Schmittlein B., Jones A. L., Ainane Y., Rizvi A., Chan D., Dickey E., Pool K., Harsono K., Szymkiewicz D., Scarfogliero U., Bhatia V., Sivanantham A., Kreciglowa N., Hunter A., Gomez M., Tanner A., Uboldi M., Batish A., Balcerek J., Kutova-Stoilova M., Paruthiyil S., Acevedo L. A., Stadnitskiy R.,·Carmichael S., Aulbach H., Hewitt M.,·De Mollerat Du Jeu X., di Robilant B., Parietti F., Esensten J.H, 2024, Development of a robotic cluster for automated and scalable cell therapy manufacturing, Cytotherapy, 26, 1095-1104. https://doi.org/10.1016/j.jcyt.2024.03.010